Ain Shams Journal of Forensic Medicine and Clinical Toxicology
January 2023, 40: 22-33

Prostatic estimation of time passed since death; oxidative stress markers, histological and immunohistochemical examination (an experimental study)

Dalia Mohamed Ali[1] Mennatallah Mahmoud Ahmed Mohamed[1],

[1] Department of Forensic Medicine and Clinical Toxicology, Faculty of Medicine-Menia University, Menia Egypt.

Abstract

Introduction: One of the most essential duties in forensic medicine is determining the postmortem interval. **Objectives:** The study's purpose is to estimate time passed since death in relation to oxidative stress markers, histopathological changes, and prostatic specific antigen in the prostate. **Methods:** Fifty mature male albino rats were classified into 5 main groups. Rats were used for determining postmortem changes and oxidative stress markers at five different postmortem intervals (0, 1, 5, 10, 15 days) with prostatic specific antigen (PSA) immunohistochemistry in the prostate. **Results:** Prostatic gland oxidant parameters (MDA, NO) revealed a significant increase while its antioxidant parameters (GSH, SOD) showed a significant decrease with increased postmortem time. The prostate gland showed normal histology at 0 hours postmortem (PM). While, at 1 day, it revealed minimal autolysis (<5%). Starting from 5 days, moderate autolysis (10–50%) was seen. Ten to fifteen days, moderate to severe autolysis (≥50%) appeared in most of the samples. Staining for PSA showed high expression (++) at 0 hours PM. Moreover, a significant decrease in the amount of PSA's stained areas that revealed low expression (+) was detected at 1 and 5 days PM. Negative (−) or no immunoreactivity for PSA has been detected at 10 and 15 days PM. **Conclusion:** Prostate-specific antigen proved to be a useful parameter consistent with the histopathological changes for the estimation of postmortem interval from the prostate. It is approved that the derived oxidative stress markers equations can be helpful in detecting the postmortem interval in forensic science.

Received in original form: 21 September 2022 Accepted in a final form: 11December 2022

Key words Postmortem interval; Oxidative stress markers; Prostatic specific antigen; Immunohistochemistry

Introduction

One of the most important duties in forensic medicine is determining the postmortem interval (PMI), or time passed since death. In the instance of a suspected death or homicide, estimation of PMI helps investigators in restructuring the circumstances (Young et al., 2013). The skill to precisely know the postmortem interval (PMI) has important implications for criminal investigations and studies. Estimating PMI is necessary for including and excluding accused based on their locations at the time of death, as well as providing a time frame within which unidentified putrefied remains could be linked to missing people (Chandrakanth et al., 2013).

After death, a complicated set of biochemical and pathological processes begin, altering the structure and content of the human body significantly. Because many of these changes happen in sequence, assessing the types and grades of change may help with PMI calculation (Ferreira and Cunha, 2013).

In any tissue injury, biochemical examination of oxidative stress markers reveals elevated lipid peroxidation markers. Malondialdehyde (MDA) is the most measured biomarker of lipid peroxidation Tissue injury shifts the natural equilibrium between antioxidant stress indicators and reactive oxygen species (ROS) in live cells in favor of ROS. The level of ROS continues to increase depending on the time after death (Welson et al., 2021).

Other contemporary approaches of PMI measurement include histological and immunohistochemical examinations of degenerative alterations in interior organs which are important because they can aid in the estimation of the PMI (Dettmeyer, 2011). A mix of conventional, biochemical, or histopathological approaches is required for accurate PMI estimation (Clarkson and Thompson, 2000).

The prostate is one of the greatest renitent organs to decomposition and post-mortem (PM) alterations, as it can be seen in a largely skeletalized cadaver for up to a year after death. As a result, the prostate is a suitable candidate for histopathological examination to determine PMI (Saukko and Knight, 2016).

We focused on the prostatic-specific antigen in this investigation (PSA). PSA is a glycoprotein with protease activity that has 237 amino acids. PSA is produced particularly in the ductal epithelial cells of the prostate gland and, when secreted in sperm, has a function in enhancing sperm motility (Tsuboi et al., 2020). PSA has been found in numerous physiological

fluids and tissues, despite being abundant in prostatic tissue and sperm so it is not particular to the prostate. PSA is discovered in female ejaculate at amounts that are similar to those found in male sperm, in addition to, high levels in breast milk and amniotic fluid (Wimpissinger et al., 2007).

In the realm of forensic medicine, however, it is well understood that the detection of PSA in sperm collected from a sexual assault victim establishes the existence of sperm. The cause of death did not affect the levels of prostate-specific antigen in postmortem serum (Tsuboi et al., 2020).

The current study aimed to evaluate time passed since death in relation to oxidative stress markers, histopathological examination, and prostatic specific antigen immunohistochemical analysis in the prostate at five different postmortem intervals (0,1, 5, 10, 15 days).

Materials and Methods

Animals

Fifty mature male albino rats weighing between 150 and 300 grams will be employed. They obtained from the Minia University laboratory animals' growth center. The animals were retained in plastic cages with suitable ventilation and sanitary conditions at normal temperature (22°C ± 5°C) under a 12:12-hour light-dark cycle., as well as having free access to balanced standard diet pellets and tap water. The experiment was conducted in accordance with the guideline of the animal use and care committee of Minia University (Approval No. 101-2021).

Experimental design

Animals were classified in 5 main groups; each contained 10 rats. After being anesthetized with ether inhalation, rats were slaughtered by cervical dislocation. During the time between death and organ removal, these rats were kept at ambient temperature and humidity (22°C, 15% relative humidity). The prostate was removed at regular intervals (0, 1, 5, 10, 15 days). For the detection of oxidative stress indicators and histological and immunohistochemical analysis, the prostate was separated into two pieces.

Tissue Preparation

To eliminate any red blood cells and clots, the prostate was perfused with a phosphate-buffered saline (PBS) solution, pH 7.4, containing 0.16 mg/ml heparin, after the animal was dissected. Tissues were then frozen at -80°C till a biochemical examination was performed.

One gramme of tissue was homogenised in 5-10 ml cold buffer (50 mM potassium phosphate, pH 7.5), then centrifuged for 15 minutes at 4000 rpm under cooling conditions. The supernatant was immediately tested.

Biochemical analysis

Malondialdehyde (MDA) level, the index of lipid peroxidation, was estimated following the method of Buege and Aust (1978). A reagent of 26 mmol/l thiobarbituric acid and 0.92 mol/l trichloroacetic acid in 0.25mol/l HCl was added to the homogenate then the supernatant was centrifuged for 10 minutes and measured at 535nm. Tetramethoxypropane was added as an external standard to prepare standard concentrations of MDA and it was repeated to prepare a standard curve. MDA was extrapolated from the corresponding absorbance using the regression line from the standard curve. The measurement unit is nmol/g.

Total nitrite/nitrate (NOx), the stable oxidation end products of nitric oxide (NO), was used as an indicator of the nitric oxide level and was assessed by the reduction of nitrate into nitrite using activated cadmium granules followed by color development with Griess reagent in an acidic medium as the method of Sastry et al. (2002). It was estimated as nmol/g.

The method for measurement of glutathione reduced concentration (GSH) was as that described by Moron et al. (1979) with a slight modification. Trichloroacetic acid (50%), was added to the homogenate and the supernatant was obtained by centrifuging for five minutes. GSH was measured by reaction with DTNB (5,5'- dithiobis, 2- nitrobenzoic acid) for five minutes and then was measured at 412 nm. It was measured in nmol/g.

The activity of Superoxide dismutase (SOD) was measured as described by Marklund and Marklund (1974) but with a slight modification. It depends on inhibition of the pyrogallol autooxidation by SOD (Marklund and Marklund, 1974). 0.2 mM pyrogallol in air-equilibrated and 50 mM tris-cacodylic acid, containing 1 mM diethylenetriaminepentaacetic acid were added to the supernatant. The rate of autoxidation was detected at 420 nm. Generally, a unit of the enzyme was defined as the amount of the enzyme that inhibited the reaction by about 50%. It was represented as U/g.

Histological analysis

Light microscopic examination

The tissue specimens of the prostatic gland were fixed in neutral buffered formalin 10%. The fixed specimens were trimmed and followed by washing and dehydrating in ascending grades of alcohol. Four to six-micrometer sections were cleared in xylene then embedded in paraffin and stained by hematoxylin and eosin according to Bancroft and Floyd (2013). By using a Nikon Eclipse microscope (50i) (Nikon Instruments Inc, Melville, NY, USA), histologic analysis was performed.

The severity of autolysis was based on the number of factors present and also the magnitude of change in the affected cells: (1)-Pyknosis,(2)-Karyorrhexis, (3)-Karyolysis, (4)-The absence of a nucleus due to complete dissolution or lysis, (5)-Cellular edema/swelling, (6)-Failure to take up stain, (7)-Intra-cytoplasmic vacuolation, (8)-Putrefaction, (9)-Altered architecture of tissue unrelated to a pathologic process (Carson and Hladik, 2009 and George et al., 2016).

Autolysis score

The evaluation and scoring of Samples by using a semi-quantitative scale in comparison to the control samples were done according to the extent of autolysis in the examined section as following minimal autolysis (<5%), mild autolysis (5–10%), moderate autolysis (10-50%), and severe autolysis (>50%) (Carson and Hladik, 2009 and George et al., 2016).

Immunohistochemical analysis

According to the previously described method, five-micrometer sections were mounted on coated slides and used for immunohistochemical staining (Suckow, Wheeler and Yan, 2009). Deparaffinized and rehydrated sections were submersed in 0.3% hydrogen peroxide for 20 min at room temperature to stop endogenous peroxidase activity. To retrieve antigen, the slides were autoclaved in a pressure cooker (21°C for 20 min) in a target retrieval solution (Dako, Cairo, Egypt). The pre-diluted primary PSA antibody (rabbit polyclonal antibody; Dako) was applied to the slides for 20 min at 35°C.

A secondary pre-diluted biotinylated immunoglobulin (Ig) link [consisting of 0.05% horse anti-mouse IgG, 0.05% goat anti-mouse IgM, 0.017% goat anti-rabbit IgG in sodium phosphate buffer (PBS) containing 0.3% carrier protein; Dako] was applied to the slides for about 20 minutes at 35°C. Then the slides were incubated with streptavidin-horseradish peroxidase for about 20 minutes at 35°C. Diaminobenzidine tetrachloride (DAB) chromogen (0.2% DAB in PBS; Dako) and DAB substrate (0.02% hydrogen peroxide in PBS; Dako) were then applied for 20 min at 35°C, followed by 4 wash solution rinses. Afterward, a copper enhancer was applied to DAB (5% cupric sulfate in deionized water) for about 20 minutes at traditional room temperature. For counterstaining, hematoxylin was applied for about 15 minutes at room temperature, followed by 4 Tris-buffer rinses and 2 wash solution rinses (Suckow, Wheeler and Yan, 2009).

To assess the PSA staining, both reviewers were blinded to the outcomes. Since there was no apparent difference in staining intensity, a three-category scoring system was modified from previous reports. High expression (++) indicates that more than 10% of cells exhibited PSA staining while low expression (+) is between 0% and 10% reactivity and negative (−) indicates that no immunoreactivity for PSA was detected. For negative control, different types of non-prostatic tissue were tested. There was no staining in positive controls when treated with non-immune sera in place of the PSA primary antibody (Nowels et al., 1988and Chen et al., 2008).

Statistical analysis

Descriptive statistics and an independent-sample t-test were done for numerical data. Pearson's correlation was also done. Simple, multiple, and multiple stepwise linear regression analyses were used to determine the equations that were used to estimate the postmortem interval. The data were analyzed by using the SPSS program (Statistical Package for Social Sciences) software (version 28).

Results

Biochemical results

Prostatic gland oxidant parameters (MDA and NO) revealed a statistically significant difference in all examined postmortem intervals (0, 1, 5, 10, 15 days) when compared all intervals with each other (Table 1, 2; Fig. 1, 2). They increased statistically with increased postmortem time. While its antioxidant parameters (GSH and SOD) showed a statistically significant difference in all postmortem intervals at 0, 1, 5, 10, and 15 days when compared together (Table 3, 4; Fig. 3,4). They decreased with increased time after death.

The correlation between the postmortem interval and prostatic oxidative stress markers is illustrated in table 5. There was a statistically significant strong positive correlation between the postmortem time and all investigated oxidant parameters (MDA and NO) in prostate tissues (Fig. 5,6). While there was a statistically significant strong negative correlation between the postmortem time and all investigated antioxidant parameters in prostate tissues (GSH and SOD) (Fig. 7,8).

For estimation of the time passed since death in the prostate of rats using the analyzed oxidative stress markers, the equations were determined by simple linear regression analysis using these parameters individually (Table 6). There was a statistically significant correlation between the time passed since death and all analyzed oxidants (MDA and NO) and antioxidants parameters (GSH and SOD). When the parameters were combined in the multiple linear regression analysis (Table 7), there was a statistically significant correlation only with MDA and time after death which was then used to develop an equation for estimation of time passed since death by the multiple stepwise linear regression analysis (Table 8).

Histopathological results

The prostatic gland of the rat group at the time of death (zero hours) showed normal histological structure (Fig. 9a). Rat's prostate gland consisted of acini and stroma (Fig. 9a). The prostatic acinar portions lined by two layers of cells, an outer layer of low cuboidal epithelium and an inner one of mucin-secreting tall columnar epithelium with inward papillary projections (Fig. 9b). The acini were surrounded by fibromuscular stroma (Fig. 9b). No significant cellular and architectural histological changes were observed and stain uptake was optimal. Normal prostatic tissue was strongly stained with antiserum to PSA. Staining for PSA was relatively uniform throughout the prostatic epithelium of the specimen, although some variation in staining intensity was noted from cell to cell (Fig. 9c). The immunostaining was restricted to the cytoplasm of prostatic epithelial cells and cell debris and secretary material within the prostatic lumina (Fig. 9c). In many cells, the apical cytoplasm was more intensely stained than were other regions of the cytoplasm High expression (++) (Fig. 9c).

The prostate gland after Twenty-four hours of death revealed minimal autolysis (<5%) appeared as disruption and swelling of the acinar epithelial lining (Fig. 10a). Faint eosinophilic acinar secretions with shrinkage of some acini were noticed (Fig. 10b). Edema of fibromuscular stroma was characterized by dispersion of fibrous tissue (Fig. 10b). Staining for PSA revealed low expression (+) of prostatic epithelial cells especially in apical cytoplasm (Fig. 10c).

The prostate gland after Day 5 of death showed moderate autolysis (10–50%) characterized by maintaining histological structural integrity with loss of

cellular details (Fig. 11a). Separation of cells by clear spaces, condensation, vacuolization, and fragmentation of the nuclei was present (Fig. 11a). Sparse distribution of mucous extra-acinar in the glandular parenchyma was showed (Fig. 11b). Marked edema of fibromuscular stroma was seen (Fig. 11b). Staining for PSA revealed low expression (+) of prostatic epithelial cells especially in apical cytoplasm (Fig. 11c).

Prostate gland after Day 10 of death showed moderate to severe autolysis (50%) of glandular architecture. Loss of acinar pattern with complete dissolution of epithelial lining nuclei was detected (Fig. 12a). Fibromuscular stroma appeared as a dense eosinophilic network that separated the autolytic acinar cell lining into a cluster (Fig. 12b). Negative (−)", no immunoreactivity for PSA was detected (Fig. 12c).

On the other side, the prostate gland after Day 15of death revealed severe autolysis (>50%) of all glandular structures including acini and fibromuscular stroma. The glandular tissue showed deterioration and putrefaction appeared as homogenous eosinophilic structureless mass (Fig. 13a). Minimal fibromuscular stroma was still seen as a very fine faint stain in-between the putrefied gland acini (Fig. 13b). Negative (−)", no immunoreactivity for PSA was detected (Fig. 13c).

Table (1): Descriptive Statistics and Independent-Sample t-Test of the analyzed malondialdehyde (oxidant parameter) between different groups depending on time after death in the prostate of rats

	Day 0	Day 1	Day 5	Day 10	Day 15	P value
	N=10	N=10	N=10	N=10	N=10	
MDA						
Range	(2.8-4.1)	(4-4.5)	(4.5-4.7)	(5.8-6.3)	(5.8-7.3)	*<0.001***
Mean ± SD	3.6±0.4	4.2±0.1	4.6±0.1	6.1±0.1	6.7±0.4	
P value						
Day 0		*<0.001***	*<0.001***	*<0.001***	*<0.001***	
Day 1			*0.002**	*<0.001***	*<0.001***	
Day 5				*<0.001***	*<0.001***	
Day 10					*<0.001***	

MDA= malondialdehyde, It was measured in nmol/g: nanomole/gram, N=number, SD=standard deviation. **: statistically highly significant, *: statistically significant, P value is significant when P <0.05.

Table (2): Descriptive Statistics and Independent-Sample t-Test of the analyzed nitric oxide (oxidant parameter) between different groups depending on time after death in the prostate of rats

	Day 0	Day 1	Day 5	Day 10	Day 15	P value
	N=10	N=10	N=10	N=10	N=10	
NO						
Range	(12.7-27.7)	(31.5-40.2)	(37.1-45.1)	(38.8-45.3)	(39-51.7)	*<0.001**
Mean ± SD	21.4±4.8	35.6±2.2	39.2±2.7	42.2±1.8	45.4±3	
P value						
Day 0		*<0.001***	*<0.001***	*<0.001***	*<0.001***	
Day 1			*0.011**	*<0.001***	*<0.001***	
Day 5				*0.036**	*<0.001***	
Day 10					*0.026**	

NO= nitric oxide, It was measured in nmol/g: nanomole/gram. N=number, SD=standard deviation. **: statistically highly significant, *: statistically significant, P value is significant when P <0.05.

Table (3): Descriptive Statistics and Independent-Sample t-Test of the analyzed glutathione reduced (antioxidant parameter) between different groups depending on time after death in the prostate of rats

	Day 0	Day 1	Day 5	Day 10	Day 15	P value
	N=10	N=10	N=10	N=10	N=10	
GSH						
Range	(263.3-294.5)	(158.4-207.2)	(132.7-156.4)	(105.2-119.5)	(85.3-104.3)	*<0.001**
Mean ± SD	279±8.9	177.2±13.7	143.3±6.3	115.4±4.3	95±6.3	
P value						
Day 0		*<0.001***	*<0.001***	*<0.001***	*<0.001***	
Day 1			*<0.001***	*<0.001***	*<0.001***	
Day 5				*<0.001***	*<0.001***	
Day 10					*<0.001***	

GSH= glutathione reduced, It was measured in nmol/g: nanomole/gram. N=number, SD=standard deviation. **: statistically highly significant, P value is significant when P <0.05.

Table (4): Descriptive Statistics and Independent-Sample t-Test of the analyzed Superoxide dismutase (antioxidant parameter) between different groups depending on time after death in the prostate of rats

	Day 0	Day 1	Day 5	Day 10	Day 15	P value
	N=10	N=10	N=10	N=10	N=10	
SOD						
Range	(30.6-66.8)	(25.6-35.4)	(22.1-25.6)	(16.1-21.2)	(10.3-13.7)	*<0.001**
Mean ± SD	52.1±10.8	30.2±2.5	23.9±1.3	17.9±1.6	12±0.9	
P value						
Day 0		*<0.001***	*<0.001***	*<0.001***	*<0.001***	
Day 1			*0.008**	*<0.001***	*<0.001***	
Day 5				*0.011**	*<0.001***	
Day 10					*0.012**	

SOD= Superoxide dismutase, it was measured in U/g: unit/gram. N=number, SD=standard deviation. **: statistically highly significant, *: statistically significant, P value is significant when P <0.05.

Table (5): Pearson's correlation coefficient for the correlation between the time after death and the analyzed oxidants and antioxidants parameters in the prostate of rats

N=50 Parameters	Time	
	R	P value
MDA	*0.959*	*<0.001***
NO	*0.784*	*<0.001***
GSH	*-0.843*	*<0.001***
SOD	*-0.812*	*<0.001***

MDA= malondialdehyde, It was measured in nmol/g: nanomole/gram. NO= nitric oxide, It was measured in nmol/g: nanomole/gram. GSH= glutathione reduced, It was measured in nmol/g: nanomole/gram. SOD= Superoxide dismutase, It was measured in U/g: unit/gram. N=number, R= Correlation coefficient "weak (r = 0-0.24), fair (r = 0.25-0.49), moderate (r = 0.5-0.74), strong (r = 0.75-1)" **: statistically highly significant, P value is significant when P <0.05.

Table (6) Simple linear regression analysis to estimate the time after death from the prostatic tissues of rats using the different analyzed oxidants and antioxidants parameters

N=50 Parameters	Unstandardized coefficients		P value	Adjusted R^2	SEE	Regression equation
	Constant	B				
MDA	-16.411	4.493	<0.001**	0.917	1.64	PMI= -16.411+ (4.493 ***x*** MDA)
NO	-12.177	0.5	<0.001**	0.606	3.57	PMI= -12.177 + (0.5 ***x*** NO)
GSH	18.002	-0.073	<0.001**	0.705	3.09	PMI= 18.002 + (-0.073 ***x*** GSH)
SOD	14.699	-0.312	<0.001**	0.653	3.35	PMI= 14.699 + (-0.312 ***x*** SOD)

MDA= malondialdehyde, It was measured in nmol/g: nanomole/gram. NO= nitric oxide, It was measured in nmol/g: nanomole/gram. GSH= glutathione reduced, It was measured in nmol/g: nanomole/gram. SOD= Superoxide dismutase, It was measured in U/g: unit/gram. N=number, R2 = effect size, SEE = standard error of estimate, PMI = postmortem interval. **: statistically highly significant, significant difference at p value < 0.05. PMI = constant + (coefficient x measured parameter) ±SEE.

Table (7): Multiple linear regression analysis to estimate the time after death from the prostatic tissues of rats using the different analyzed oxidants and antioxidants parameters

N=50 Parameters	Unstandardized coefficients		P value	Adjusted R^2	SEE	Regression equation
	Constant	B				
MDA	-14.478	4.132	<0.001**	0.914	1.67	PMI= -14.478 + (4.132 ***x*** MDA) + (0.020 ***x*** NO) + (-0.005 ***x*** GSH) + (-0.001 ***x*** SOD)
NO		0.020	0.794			
GSH		-0.005	0.737			
SOD		-0.001	0.981			

MDA= malondialdehyde, It was measured in nmol/g: nanomole/gram. NO= nitric oxide, It was measured in nmol/g: nanomole/gram. GSH= glutathione reduced, It was measured in nmol/g: nanomole/gram. SOD= Superoxide dismutase, It was measured in U/g: unit/gram. N=number, R2 = effect size, SEE = standard error of estimate, PMI = postmortem interval. **: statistically highly significant, significant difference at p value < 0.05.

Table (8): Multiple stepwise linear regression analysis to estimate the time after death from the prostatic tissues of rats using the malondialdehyde parameter

N=50 Parameters	Unstandardized coefficients		P value	Adjusted R^2	SEE	Regression equation
	Constant	B				
MDA	-16.411	4.493	<0.001**	0.917	1.64	PMI= -16.411 + (4.493 *x* MDA)

MDA= malondialdehyde, It was measured in nmol/g: nanomole/gram. N=number, R2 = effect size, SEE = standard error of estimate, PMI = postmortem interval. **: statistically highly significant, significant difference at p value < 0.05. Stepwise discriminant analysis revealed one model for postmortem time estimation from oxidant parameter which is the MDA

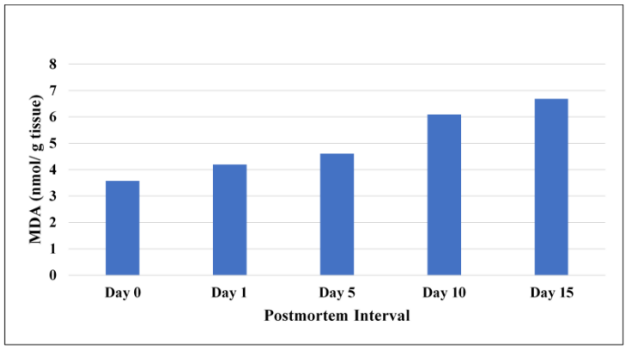

Figure (1): Statistical analysis of malondialdehyde (MDA) levels demonstrated a significant increase in its levels with increase the examined postmortem interval.

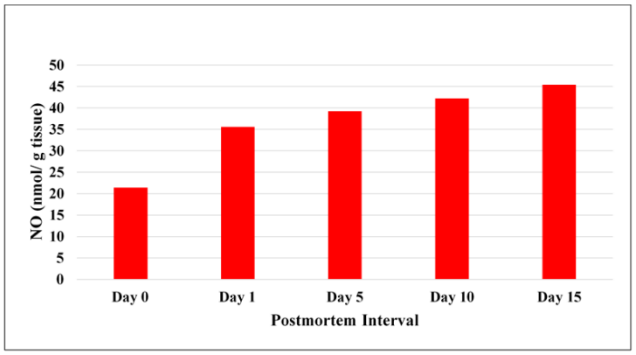

Figure (2): Statistical analysis of nitric oxide (NO) levels demonstrated a significant increase in its levels with increase the examined postmortem interval.

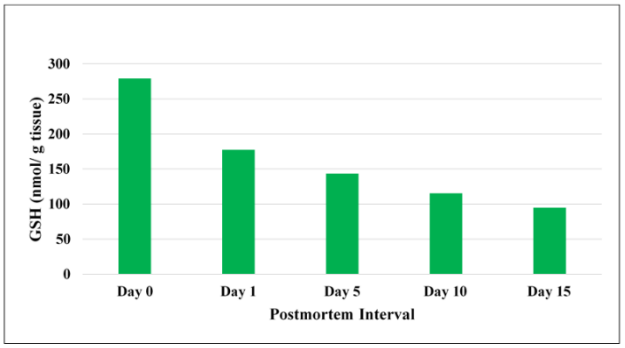

Figure (3): Statistical analysis of glutathione reduced (GSH) levels demonstrated a significant decrease in its levels with increase the examined postmortem interval.

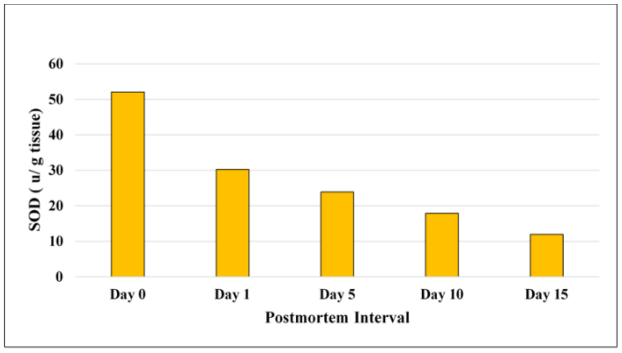

Figure (4): Statistical analysis of Superoxide dismutase (SOD) levels demonstrated a significant decrease in its levels with increase the examined postmortem interval.

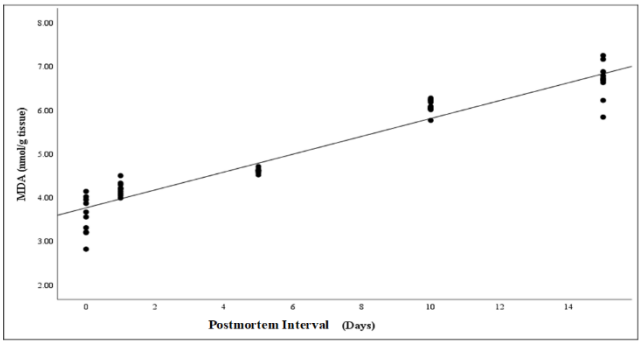

Figure (5): Regression curve showing correlation between malondialdehyde (MDA) level and different postmortem time.

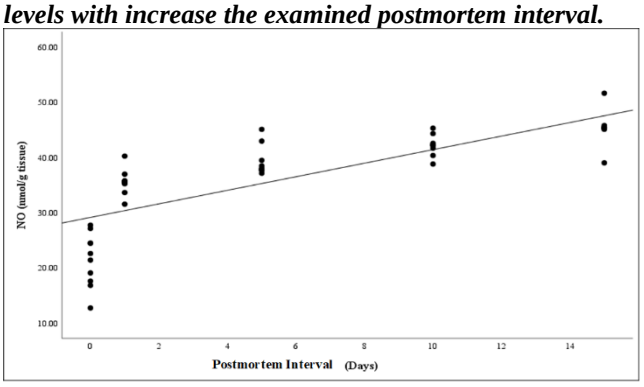

Figure (6): Regression curve showing correlation between nitric oxide (NO) level and different postmortem time.

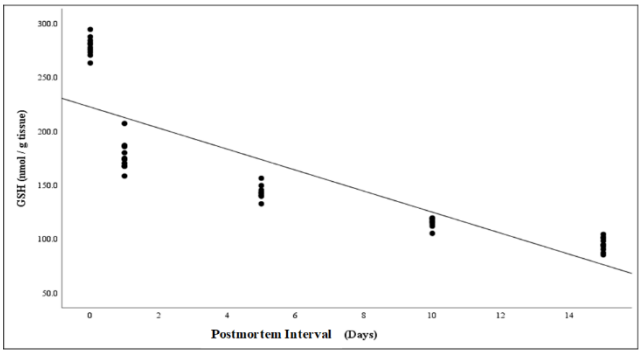

Figure (7): Regression curve showing correlation between glutathione reduced (GSH) level and different postmortem time.

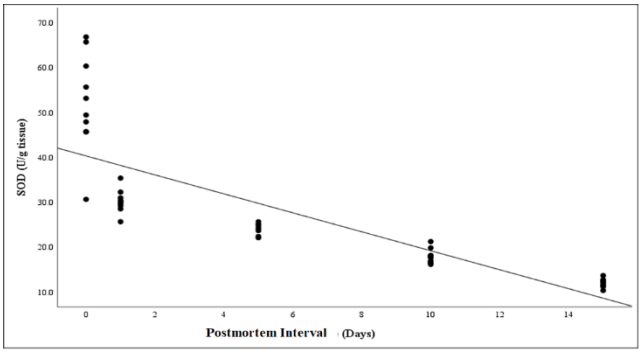

Figure (8): Regression curve showing correlation between Superoxide dismutase (SOD) level and different postmortem time.

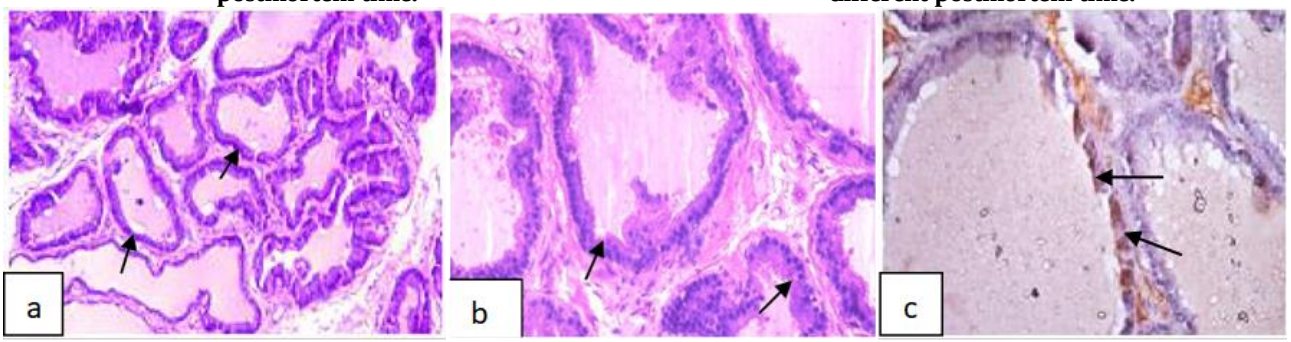

Figure (9): Photomicrograph of prostate gland showing [day 0] (a) Normal histological structure of prostate gland consisted of acini and stroma (arrow) (H&Ex200). (b) Acini lined by an outer low cuboidal layer and an inner layer of tall columnar and surrounded by fibromuscular stroma (arrow) (H&Ex400). (c) High expression of PSA immunostained for apical cytoplasm of acinar epithelial lining (arrow) (PSA immune-stainx400).

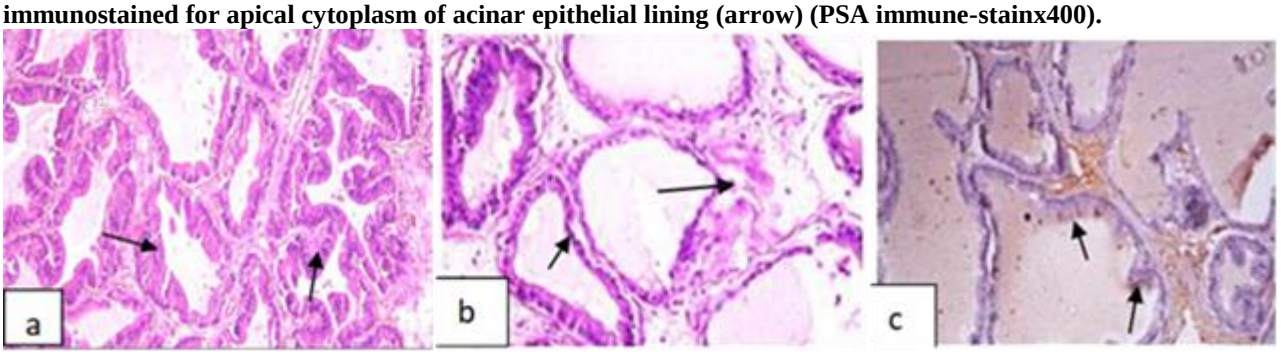

Figure (10): Photomicrograph of prostate gland showing [day 1] (a) Disruption and swelling of acinar epithelial lining (arrow) (H&Ex200). (b) Faint eosinophilic acinar secretions with shrinkage of some acini and edema of fibromuscular stroma (arrow) (H&Ex400). (c) Low expression of PSA immunostained for prostatic acinar epithelial cells (arrow) (PSA immunestainx400).

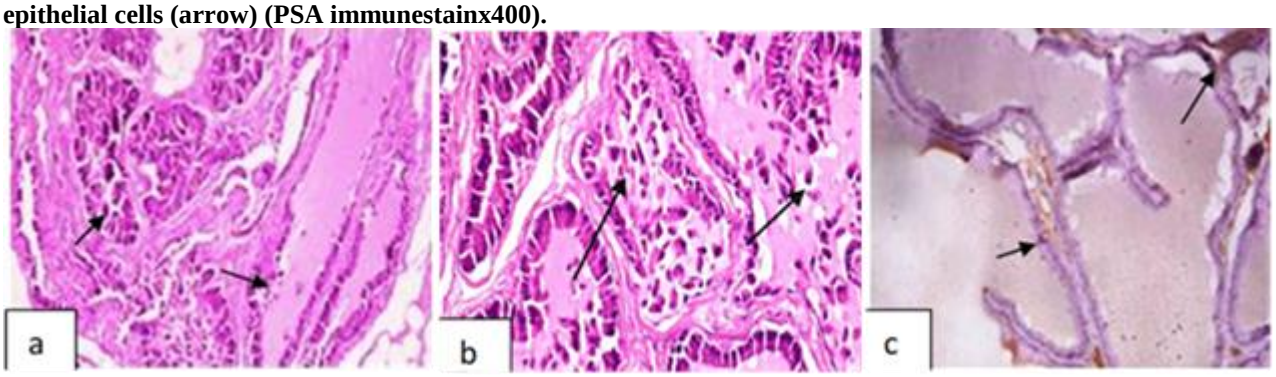

Figure (11): Photomicrograph of prostate gland showing [day 5] (a) Cellular separation by clear spaces, vacuolization and loss of cellular details (arrow) (H&Ex200). (b) Mucous extra-acinar sparsely distributed in the glandular parenchyma. (c) Low expression of PSA immunostained for prostatic acinar epithelial cells (arrow) (PSA immunestainx400).

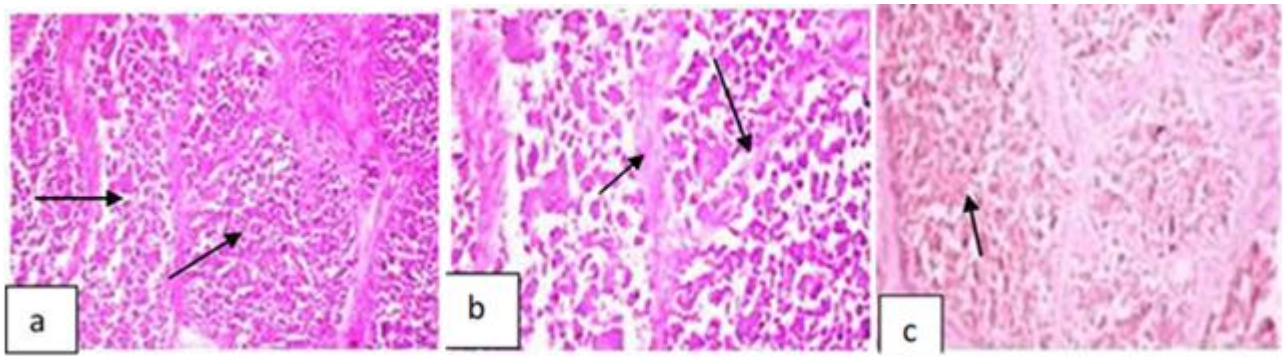

Figure (12): Photomicrograph of prostate gland showing [day 10] (a) Losses of aciner pattner with complete dissolution of epithelial lining nuclei (arrow) (H&Ex200). (b) Fibromuscular stroma as dense eosinophilic network separated the autolytic acinar cell lining into cluster (arrow) (H&Ex400). (c) Negative expression of PSA immunostained for prostatic acinar epithelial cells (arrow) (PSA immunestainx400).

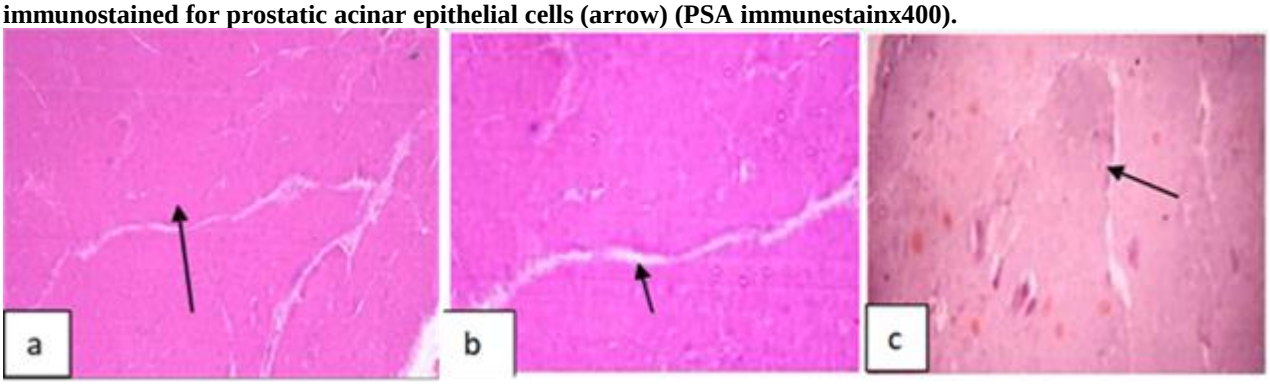

Figure (13): Photomicrograph of prostate gland showing [day 15] (a) Deterioration and putrefaction of glandular tissue which appeared as homogenous eosinophilic structurless mass (arrow) (H&Ex200). (b) Minimal fibromuscular stroma as very fine faint stain in-between the putrefied gland acini (arrow) (H&Ex400). (c) Negative expression of PSA immunostained for prostatic acinar epithelial cells (arrow) (PSA immunestainx400).

Discussion

The prostate gland has a low concentration of hydrolytic enzymes in its cells so it is more resistant and takes a long time to decompose as the autolytic process is more prominent in the organs with a high concentration of hydrolytic cellular enzymes (Almulhim and Menezes, 2021). There is a restricted number of microorganisms that have a collagenolytic activity that is needed for the degradation of the collagen coating of the prostate gland which explained its resistance to decay (Lutz et al., 2020). For these reasons, the prostate gland was used for the estimation of postmortem interval in the present study.

In the current study, the levels of MDA and NO at 10 and 15 day PM were two times as greater as the level at the immediate time of death (0 postmortem). While the amount of SOD decreased at 10 and 15 day PM to a level which was three to four times as less as the level at the time of death and GSH decreased to three times as less as that at 0 hour PM. This means that, the decline in SOD and GSH activities is independent of the increase in MDA and NO levels. Kurt et al. (2011) and Polat et al. (2011) observed that the antioxidant activity in the damaged experimental tissues decreases in the normal conditions to a level that is half as much as that in the healthy subjects which explains the present findings.

Malondialdehyde (MDA) is a toxic aldehyde that releases through peroxidation of the fatty acids containing three or more double bonds (Niki et al., 2005 and Yaman and Ayhanci, 2021). Nitric oxide(NO) is an endogenous mediator in various physiological processes as it regulates vascular relaxation, protein, and gene expression changes, and also regulates cellular inflammatory function (Repetto, Semprine and Boveris, 2012). Similar to what was reported in the current study that MDA and NO activities increased significantly with the increase of postmortem time, it was reported in the experimental studies that the concentration of oxidants increased in parallel to the increase in the range of damage (Celik et al., 2004 and Ozturk et al., 2013).

Superoxide dismutase (SOD) is one of the most powerful endogenous antioxidants which acts by converting the free radicals into harmless compounds or by inhibiting their formation (Ighodaroab and Akinloyeb, 2018). Glutathione reductase (GSH) is another important antioxidant that is protecting the cells from oxidative damage (Yilmaz et al., 2012).

An increase in oxidants and a decrease in antioxidant amounts are detected in the damaged tissues (Iraz et al., 2006). After death, the oxidant/antioxidant balance is insufficiently controlled

by the body (Aguilar et al., 2007). The increase in the levels of MDA with increasing PMI is due to the increase in the lipid peroxidation that is detoxified by GSH which is vastly reduced (Harish et al., 2011).

By using regression analysis, the equations were developed for postmortem interval estimation. In the prostate, the less the standard error of estimate (SEE), the more significant predictor that was found to be MDA followed by GSH then SOD and lastly NO. Otherwise, Sener et al. (2012) revealed that SOD and NO were the most significant parameters affecting the prediction of the postmortem interval in the rat liver.

There are different researches that documented the successive role of oxidant and antioxidant markers in estimating the postmortem interval from different organs. Abo El-Noor et al. (2016) proved that there was a significant correlation between oxidative stress markers in the heart and kidney and the postmortem interval. Oxidant and antioxidant parameters are best correlated to postmortem time in the heart and kidney as well as testis as suggested by Welson et al. (2021). Ozturk et al. (2013) who conducted a study in the femoral muscle, also reported a significant increase in the oxidants and a decrease in the antioxidants 2 hours after death.

Shaaban et al. (2017), in the same line, studied the role of oxidant and antioxidant parameters in the estimation of PM interval, observed that there was a significant rise in the levels of MDA and NO and a significant decline in the levels of GSH and SOD in brain and liver of rats after 8 hours of death. Their results differ from the present study in the early affection of oxidative stress markers in the early postmortem time. These enzymes differ in their responses because of the different nature, amount, and activities of the enzymes in the different organs (Szymonik-Lesiuk et al., 2003).

The current study comes in conjunction with what was mentioned by Mahmoud et al. (2018) who revealed that there was not any structural abnormality occurred in the prostate during the first 12 hours of death but significant disruption of epithelial lining with presence of inflammatory cells appeared in the prostatic gland after 24 hours PM. More degenerative changes of the prostatic acini occurred one to four weeks PM. They also concluded that these changes can successively be used as a predictor for estimation of postmortem time.

The current results come in an agreement with what was stated by Elgawish et al. (2021) whose study revealed that the prostate samples didn't show any structural abnormalities during the first 12 hours. It was also revealed that after 24 hours PM, desquamation of the epithelium with the appearance of inflammatory cells was detected then atrophic prostatic tissues with necrosis were observed at 60 to 72 hours PM.

The current histopathological results disagree with what was stated by Saukko and Knight (2016) as they reported that the human prostate gland may still be identifiable in a partially skeletonized human body for about one year PM. The accelerated degradation rate of the rat prostate gland in the current study can be explained by the smaller size of rats' prostate in comparison to the prostate of human beings and also by the difference in the lining of prostatic epithelium which is simple columnar epithelium in the rats' prostate compared to the pseudostratified and stratified columnar epithelium in the human prostate that is more resistant (Aaron, Franco and Hayward, 2016).

The rapid degradation rate of the prostate gland in the present study may also be attributed to the mass of the carcass which is the most important intrinsic factor that affects the postmortem decomposition rate and therefore the estimation of postmortem interval. The bodies of small masses decomposed more rapidly than those of large masses (Matuszewski et al., 2014).

The results of the current study revealed that there was a positive high immunoreactivity expression of PSA in the prostatic tissues at 0 PM. A significant decrease in the concentration of PSA's stained areas in the prostate was detected with an increase in the PMI. They also revealed a presence of positive low expression of PSA in the prostate at 1 and 5 days PM while at 10 and 15 days, immune-histochemical reaction for PSA was absent in all prostatic acini.

Jones et al. (2005) revealed that the total serum PSA levels were similar before and after death if blood autopsy was drawn in the first 24 hours after the time of death. While the free serum PSA levels were increased two times in postmortem sera as greater as antemortem sera that were analyzed.

Furthermore, Forde et al. (2016) concluded that there is no significant difference in the levels of serum PSA levels that were examined at various intervals (4, 8, 24, 48 hours). But we cannot compare the current results with that study because they examined PSA levels in the blood collected from living patients and then they left specimens for various intervals.

Tsuboi et al. (2020) found that there was no statistically significant correlation between serum PSA levels and postmortem interval whether regardless of age at death or with considered the age of cadavers. They revealed that PSA is a stable material that is not affected by the putrefaction or the environment of the corpses.

Conclusion

The present study concluded that prostate-specific antigen proved to be a useful indicator consistent with the histopathological findings in the estimation of postmortem interval from the prostate. There is a strong relationship between oxidative stress markers and time after death and it is approved that the derived equations in this study can be helpful in detecting the postmortem interval in forensic science.

Recommendations

Although the prostate withstands decomposition for a long period, the researches that investigate the role of postmortem changes of the prostate in the estimation of also postmortem interval are lacking. So, it is recommended to do future studies on the prostate to appreciate its beneficial role in the estimation of time passed after death. Also, it is recommended to apply this study to humans to confirm whether the resulted

equations could be applied for the estimation of postmortem interval. The effects of the postmortem autolytic process-related factors are not investigated in the current study, so further studies are recommended to evaluate these factors.

Acknowledgments

The authors thank Prof. Dr. Ahmed Hassan Osman, Pathology Department, Cairo University for his efficient assistance and great effort in the histopathological study in this work. Many thanks to Dr. Mostafa Mohamed Asem for statistical analysis perform.

References

Aaron L, Franco OE & Hayward SW (2016): Review of prostate anatomy and embryology and the etiology of benign prostatic hyperplasia. Urol. Clin. North Am., 43(3):279-88. DOI: 10.1016/j.ucl.2016.04.012.

Abo El-Noor MM, Elhosary NM, Khedr NF & El-Desouky KI (2016): Estimation of early postmortem interval through biochemical and pathological changes in rat heart and kidney. Am. J. Forensic Med. Pathol., 37(1):40-6. DOI: 10.1097/PAF.0000000000000214.

Aguilar A, Alvarez-Vijande R, Capdevila S, Alcoberro J & Alcaraz A (2007): Antioxidant patterns (superoxide dismutase; glutathione reductase; and glutathione peroxidase) in kidneys from non-heart beating-donors: experimental study. Transplant. Proc., 39(1):249-52. DOI: 10.1016/j.transproceed.2006.10.212.

Almulhim AM & Menezes RG (2021): Evaluation of Postmortem Changes. In Stat Pearls; Stat Pearls Publishing: Treasure Island, FL, USA, 2021.

Bancroft JD & Floyd AD (2013): Light microscopy. In: Bancroft's Theory and Practice of Histological Techniques (7th ed.). Edinburgh, London, Melbourne, New York: Churchill Livingstone, Ch. 3; 37-68.

Buege JA & Aust SD (1978): Microsomal lipid peroxidation. Methods in enzymology, 52:302-10. DOI: 10.1016/s0076-6879(78)52032-6.

Carson FL & Hladik C (2009): Histotechnology: a self-instructional text (3rd ed.). Hong Kong: American Society for Clinical Pathology Press.

Celik O, Turkoz Y, Hascalik S, Hascalik M, Cigremis Y, Mizrak B et al. (2004): The protective effect of caffeicacid phenethyl ester on ischemia-reperfusion injury in rat ovary. Eur. J. Obstet. Gynecol. Reprod. Bio., 117(2):183-8. DOI: 10.1016/j.ejogrb.2004.05.007.

Chandrakanth HV, Kanchan T, Balaraj BM, Virupaksha HS & Chandrashekar TN (2013): Postmortem vitreous chemistry--an evaluation of sodium; potassium and chloride levels in estimation of time since death (during the first 36h after death). J. Forensic Leg. Med., 20(4): 211-6. DOI: 10.1016/j.jflm.2012.09.001.

Chen JC, Ho CL, Tsai HW, Tzai TS, Liu HS, Chow NH et al. (2008): Immunohistochemical Detection of Prostate-specific Antigen Expression in Primary Urothelial Carcinoma of the Urinary Bladder. Anticancer Research, 28(6B):4149-54.

Clarkson PM & Thompson HS (2000): Antioxidants: what role do they play in physical activity and health?. Am. J. Clin. Nutr., 72(2 Suppl):637S-46S. DOI: 10.1093/ajcn/72.2.637S.

Dettmeyer R (2011): Staining techniques and microscopy. In: Forensic Histopathology Fundamentals and Perspectives. Berlin: Springer, 17-35.

Elgawish RA, Abdelrazek HM, Desouky A & Mohamed RM (2021): Determination of postmortem interval through histopathological alterations and collagen evaluation in the prostate of Wistar albino rats. Zagazig J. Forensic Med. & Toxicology, 19(2):1-12. DOI: 10.21608/zjfm.2021.63677.1071.

Ferreira MT & Cunha E (2013): Can we infer post mortem interval on the basis of decomposition rate? A case from a Portuguese cemetery. Forensic Science International, 226(1-3):298.e1-6. DOI: 10.1016/j.forsciint.2013.01.006.

Forde JC, Blake O, Crowley VE & Lynch TH (2016): Stability and accuracy of total and free PSA values in samples stored at room temperature. Ir. J. Med. Sci., 185(4):989-91. DOI: 10.1007/s11845-015-1364-8.

George J, Van Wettere AJ, Michaels BB, Crain D & Lewbart GA (2016): Histopathologic evaluation of postmortem autolytic changes in bluegill (Lepomis macrohirus) and crappie (Pomoxis anularis) at varied time intervals and storage temperatures. Peer J., 4(e1943):1-13. DOI: 10.7717/peerj.1943.eCollection 2016.

Harish G, Venkateshappa C, Mahadevan A, Pruthi N, Srinivas Bharath MM & Shankar SK (2011): Glutathione metabolism is modulated by postmortem interval; gender difference and agonal state in postmortem human brains. Neurochemistry International, 59(7):1029-42. DOI: 10.1016/j.neuint.2011.08.024.

Ighodaroab OM & Akinloyeb OA (2018): First line defence antioxidants-superoxide dismutase (SOD), catalase (CAT) and glutathione peroxidase (GPX): Their fundamental role in the entire antioxidant defence grid. Alexandria Journal of Medicine, 54(4):287-93. DOI: org/ 10. 1016/j.ajme.2017.09.001.

Iraz M, Ozerol E, Gulec M, Tasdemir S, Idiz N, Fadillioglu E et al. (2006): Protective effect of caffeic acid phenethyl ester (CAPE) administration on cisplatin-induced oxidative

damage to liver in rat. Cell. Biochem. Funct., 24(4): 357-61. DOI: 10.1002/cbf.1232.

Jones RF, Sunheimer R,Friedman H, Miller D, Ginsburg R, Jumbelic M et al. (2005): Comparison of Ante- and Post-Mortem PSA Levels for Epidemiological Studies. Anticancer Research. 2005; 25(2B):1263-8.

Kurt A, Isaoglu U, Yilmaz M, Calik M, Polat B, Hakan H et al. (2011): Biochemical and histological investigation of famotidine effect on postischemic reperfusion injury in the rat ovary. J. Pediatr. Surg., 46(9):1817-23. DOI: 10. 1016/ j. jpedsurg.2011.04.092.

Lutz H, Vangelatos A,Gottel N, Osculati A, Visona S, Finley SJ et al. (2020): Effects of Extended Postmortem Interval on Microbial Communities in Organs of the Human Cadaver. Front. Microbiol., 11:569630 pp. 1-11. DOI: 10. 3389/ fmicb.2020.569630.eCollection 2020.

Mahmoud NA, Hassan AA, Abdel Rahim AH, Abdel Rahim AH, Suzan Mostafa Mahmoud SM & Nada OH (2018): Molecular versus histopathological examination of the prostate gland in the estimation of post-mortem interval (an experimental study). Egypt. J. Forensic Sci. Appli. Toxicol., 18(1):35-54. DOI: 10. 21608/ ejfsat.2018.28293.

Marklund S & Marklund G (1974): Involvement of the superoxide anion radical in the autoxidation of pyrogallol and a convenient assay for superoxide dismutase. Eur. J. Biochem., 47(3):469-74. DOI: 10.1111/j.1432-1033.1974.tb03714.x.

Matuszewski S, Konwerski S, Frątczak K & Szafałowicz M (2014): Effect of body mass and clothing on decomposition of pig carcasses. Inter. J. Legal Med., 128(6):1039-48. DOI: 10.1007/s00414-014-0965-5.

Moron MS, Depierre JW & Mannervik B (1979): Levels of glutathione, glutathione reductase and glutathione S-transferase activities in rat lung and liver. Comparative Study. Biochim. Biophys. Acta., 582(1):67-78. DOI: 10. 1016/ 0304-4165(79)90289-7.

Niki E, Yoshida Y, Saito Y & Noguchi N (2005): Lipid peroxidation: mechanisms, inhibition, and biological effects. Biochem. Biophys. Res. Commun., 338(1):668-76. DOI: 10. 1016/ j. bbrc. 2005. 08.072. Epub 2005 Aug nineteen.

Nowels k, Kent E, Rinsho K & Oyasu R (1988): Prostate-specific antigen and acid phosphatase-reactive cells in cystitis cystica and glandularis. Arch. Pathol. Lab. Med., 112(7):734-7.

Ozturk C, Sener MT, Sener E, Yilmaz I, Akcay F & Suleyman H (2013): The Investigation of Damage in the Muscle Tissue with the Oxidant/Antioxidant Balance and the Extent of Postmortem DNA Damage in Rats. Life Sci. J., 10(3):1631-7.

Polat B, Albayrak Y, Suleyman B, Dursun H, Odabasoglu F, Yigiter M et al. (2011): Antiulcerative effect of dexmedetomidine on indomethacin-induced gastric ulcer in rats. Pharmacol. Rep., 63(2):518-26. DOI: 10. 1016/ s1734-1140(11)70518-7.

Repetto M, Semprine J & Boveris A (2012): Lipid Peroxidation: Chemical Mechanism, Biological Implications and Analytical Determination. Available from: https://www.intechopen.com/ chapters/ 38477. Lipid Peroxidation, Angel Catala, IntechOpen, DOI: 10.5772/45943; 2012.

Sastry K, Moudgal R, Mohan J, Tyagi JS & Rao GS (2002): Spectrophotometric determination of serum nitrite and nitrate by copper-cadmium alloy. Anal. Biochem., 306(1):79-82. DOI 10. 1006/ abio. 2002.5676.

Saukko P & Knight B (2016): The Pathophysiology of death. In: Knight's Forensic pathology (4th ed.). Boca Raton, Florida: CRC press Taylor and Francis group, Ch. 2; 54-95.

Sener MT, Suleyman H, Hacimuftuoglu A, Polat B, Cetin N, Suleyman B et al. (2012): Estimating the postmortem interval by the difference between oxidant/antioxidant parameters in liver tissue. Adv. Clin. Exp. Med., 21(6):727-33.

Shaaban AA, Farrag IM & Bayoumy ES (2017): Estimation of early postmortem interval by biochemical changes in brain and liver of rats using some oxidant and antioxidant parameters. Egypt J. Forensic Sci. Appli. Toxicol., 17(1): 147-62. DOI: 10. 21608/ ejfsat. 2017. 46108.

Suckow MA, Wheeler J & Yan M (2009): PAIII prostate tumors express prostate specific antigen (PSA) in Lobund-Wistar rats. Can. J. Vet. Res., 73(1):39-41.

Szymonik-Lesiuk S, Czechowska G, Stryjecka-Zimmer M, Słomka M, Madro A, Celinski K et al. (2003): Catalase; superoxide dismutase;and glutathione peroxidase activities in various rat tissues after carbon tetrachloride intoxication. J. Hepatobiliary Pancreat. Surg., 10(4):309-15. DOI: 10.1007/s00534-002-0824-5.

Tsuboi H, Miyamori D,Ishikawa N, Ichioka H & Ikegaya H (2020):Relationship between serum prostate-specific antigen and age in cadavers. SAGE Open Medicine, 8:1-7. DOI: 10.1177/2050312120958212.

Welson NN, Gaber SS, Batiha GE & Ahmed SM (2021): Evaluation of time passed since death by examination of oxidative stress markers, histopathological, and molecular changes of major organs in male albino rats. International Journal of Legal Medicine, 135(1):269-80. DOI: 10.1007/s00414-020-02463-1.

Wimpissinger F, Stifter K, Grin W & Stackl W (2007): The female prostate revisited: Perineal ultrasound and biochemical studies of female ejaculate. J. Sex. Med., 4(5):1388-93. DOI: 10.1111/j.1743-6109.2007.00542.x.

Yaman SO & Ayhanci A (2021): Lipid Peroxidation [Online First], IntechOpen, Offered from: https://www.intechopen.com/online-first/75229. DOI: 10.5772/intechopen.95802; 2021.

Yilmaz M, Isaoglu U, Cetin N, Turan MI, Suleyman B, Gocer F et al. (2012): Effects of adrenalin on ovarian injury formed by ischemia reperfusion in rats. Latin American Journal of Pharmacy, 31(7):1032-7.

Young ST, Wells JD, Hobbs GR & Bishop CP (2013): Estimating postmortem interval using RNA degradation and morphological changes in tooth pulp. Forensic Science International, 229(1-3)163.e1-6. DOI: 10. 1016/ j. forsciint. 2013.03.035.

تقدير البروستاتا للوقت المنقضي منذ الوفاة، علامات الأجهاد التأكسدي، الفحص النسيجي والكيميائي المناعي (دراسة تجريبية)

داليا محمد علي[١] و منة الله محمود أحمد محمد[١]

الملخص العربي

المقدمة: واحدة من أهم واجبات الطب الشرعي هى تحديد فترة ما بعد الوفاة. **الأهداف:** الغرض من الدراسة هو تقدير الوقت المنقضي منذ الوفاة فيما يتعلق بعلامات الأجهاد التأكسدي، التغييرات النسيجية المرضية و مستضد البروستات النوعي فى البروستاتا.

الطرق: تم تصنيف خمسين جرذا ناضجا من ذكور الجرذان البيضاء الي ٥ مجموعات رئيسية. تم استخدام الجرذان لتحديد التغيرات بعد الوفاة وعلامات الأجهاد التأكسدي في خمس فترات مختلفة بعد الوفاة (٠ ، ١ ، ٥ ، ١٠ ، ١٥ أيام) مع الكيمياء المناعية لمستضد البروستات النوعي ((PSA فى البروستاتا.

النتائج: اظهرت معاملات أكسدة (MDA,NO) غدة البروستات زيادة معنوية فى حين أظهرت معاملاتها المضادة للأكسدة (GSH,SOD) انخفاضا معنويا مع زيادة الوقت بعد الوفاة. أظهرت غدة البروستات انسجة طبيعية فى ٠ ساعات بعد الوفاة ((PM. بينما، فى يوم واحد، كشف عن الحد الأدني من التحلل الذاتى (<٥%). ابتداء من ٥ أيام، شوهد انحلال ذاتي متوسط (١٠–٥٠%). من عشرة الي خمسة عشر يوماً، ظهر انحلال ذاتي متوسط الى شديد (≤٥٠%) في معظم العينات. أظهر تلطيخ PSA تعبيراً عالياً (++) فى ٠ ساعات بعد الوفاة PM. علاوة على ذلك، تم الكشف عن انخفاض كبير فى كمية المناطق الملطخة ب PSA التي أظهرت تعبيراً منخفضاً (+) فى ١ و ٥ أيام بعد الوفاة PM. تم اكتشاف نشاط مناعي سلبي (-) أو معدوم ل PSAفى ١٠ و ١٥ يوما بعد الوفاة PM.

الخلاصة: ثبت أن مستضد البروستاتا النوعى هو معامل مفيد يتفق مع التغيرات النسيجية المرضية لتقدير الفاصل الزمني بعد الوفاة من البروستاتا. تمت الموافقة علي أن معادلات علامات الأجهاد التأكسدي المشتقة يمكن أن تكون مفيدة في اكتشاف فترة ما بعد الوفاة في علم الطب الشرعي.

١. قسم الطب الشرعي والسموم الاكلينكية، كلية الطب البشري، جامعة المنيا، مصر.